217

FEM simulation of a full-scale loading-to-failure test of a corrugated steel culvert

Amer Wadi [*1,3], Lars Pettersson [2a] and Raid Karoumi [1b]

[1] *Division of Structural Engineering and Bridges, KTH Royal Institute of Technology, SE-100 44, Stockholm, Sweden*
[2] *Skanska Sweden AB - Major Projects, SE-112 74, Stockholm, Sweden*
[3] *ViaCon AB, SE-531 02, Lidköping, Sweden*

Abstract. This paper utilizes 3D FEM to provide deeper insights about the structural behaviour of a 6.1 m span steel culvert, which was previously tested under extreme loading. The effect of different input parameters pertaining to the backfill soil has been investigated, where the structural response is compared to field measurements. The interface choice between the steel and soil materials was also studied. The results enabled to realize the major influence of the friction angle on the load effects. Moreover, the analyses showed some differences concerning the estimation of failure load, whereas reasons beyond this outcome were arguably presented and discussed.

Keywords: flexible culvert; soil-steel composite bridge; corrugated steel; finite element model; ultimate limit state; failure test

1. Introduction

Flexible culverts are becoming widely used as economical alternatives to similar traditional concrete structures. Their best advantage is in their construction time saving and the implied simplicity in the assembly process. For that reason, practitioners are frequently interested to expand their use toward larger spans and structures with shallower soil covers. Yet, the complex nature of the interaction between the soil and the steel materials marks a special challenge for practitioners, where research is constantly stimulated to seek for the true capacity of these structures. Since the birth of the ring compression theory (White L and Layer P 1960), different design methods have been developed to account for the various design conditions and facilitate the use of larger spans. Several field and lab tests were performed throughout the years to realize the behaviour of flexible culverts (also known as soil–steel composite bridges, SSCB) and their performance in different conditions (Klöppel and Glock 1970, Temporal *et al.* 1985, Kunecki and Kubica 2004, Pettersson 2007, Bayoğlu Flener and Karoumi 2009, Brachman *et al.* 2010, Beben 2013, Elshimi *et al.* 2013, Mellat *et al.* 2014, Simpson *et al.* 2015, Regier *et al.* 2017). These tests together with the use of computer simulations (i.e., FEM) have allowed researchers to reflect their findings in the development process of the different design methods.

Currently, there are several design methods being used in North America and Europe (AASHTO 2012, CSA Canadian Standards Association 2014, Pettersson *et al.* 2015), which were developed and tailored to reflect the state of the art and to represent country's specific requirements for the design and construction.

The use of FEM has helped researchers in realizing the structural behaviour of SSCB, where several investigations have been carried out by modelling SSCB both in 2D and 3D simulation environments. This has included the structural response under soil load (i.e., backfilling) and live loads as well. A fair summary of these FEM efforts were presented by Elshimi (2011). In fact, the soil culvert interaction (SCI) by Duncan (1978, 1979) has utilized 2D FEM results to propose a set of design equations, where they subsequently formed the bases of Canadian Highway Bridge Design Code (CHBDC) (CSA Canadian Standards Association 2014) and Swedish design method (SDM) (Pettersson and Sundquist 2014, Pettersson *et al.* 2015). In addition, the research presented in (Moore and Taleb 1999, McGrath *et al.* 2002), which compiled the study efforts for a 9.5 m span metal arch culvert field test together with FEM, gave the opportunity to provide recommended specifications for large-span culverts. These proposed modifications were adopted in the AASHTO design method (AASHTO 2012).

One of the recent efforts to predict the ultimate capacity of SSCB was presented by Brachman *et al.* (2010) and Elshimi (2011) for a 10.1 m span tested box culvert, where the research indicated the potential use of 3D FEM for the prediction of the ultimate capacity. Other 3D studies did not specifically deal with the ultimate capacity of SSCB but rather covered the in-service loading conditions. These 3D efforts covered different topics and mostly assumed fully

---

∗Corresponding author, Ph.D. Student,
 E-mail: wadi@kth.se
[a] Professor
[b] Professor

elastic models, had a limited sensitivity study on the assumed soil parameters, assumed simplified orthotropic steel plates or had less focus on the effect of soil–steel interface on the structural performance (Moore and Brachman 1994, Moore and Taleb 1999, El-Sawy 2003, Mellat *et al.* 2014, Yeau *et al.* 2014, Beben and Stryczek 2016, Beben and Wrzeciono 2017). In this context, the developments in FEM simulations allow practitioners to perceive deeper insights about the complex interaction between the soil and steel materials and help to realize the influence of the different factors on the structural performance. In particular, the advances in the 3D modelling will surely supplement the knowledge concerning the true bearing capacity of these structures. Furthermore, the accurate estimation of load effects (soil and live load) including normal forces and bending moments certainly help designers to provide more reliable designs in fulfilling the current market challenges for larger spans and shallower covers.

1.1 Aim and scope

This study aims to provide deep insights about the structural behaviour of SSCB using 3D FEM simulation. The ultimate capacity of an earlier tested 6.1 m pipe arch is analysed using a 3D simulation environment, where the simulation intends to examine the ultimate bearing capacity for the case of having an axle load placed above the crown. The effect of different input parameters (mainly the backfill soil) on the structural response is investigated and discussed, where FEM results are analysed and compared to the field measurements. Given the nature of the problem, the 3D modelling was selected to reasonably capture the live load distribution through the soil and to be able to model the orthotropic behaviour of the steel corrugation in the most realistic manner. Live load deformation, the distribution of normal forces and bending moments along the pipe circumference are studied. In addition, live load stresses in soil and the mode of failure of the structure are also underlined and discussed. While this investigation assumes primarily frictional interface between the soil and steel (compare Section 3.3), the effect of a tied and a frictionless interfaces was also highlighted and briefly discussed. It should be noted that although bolted connections are typically a main feature of these structures, they were not included in the simulations. The behaviour of the bolted connection itself is believed of a complex nature and rightly requires dedicated studies. Hence, to avoid further complexity, the pipe was modelled as continuous corrugated steel wall (see also Section 3.3).

2. The case study

Although many culverts have been tested under live loads, there are very few full-scale field tests, where metal culverts are actually loaded to failure. In recent years, for reasons believed to their unique shape, the ultimate capacity of box culverts were investigated, where 8 m (Bayoglu Flener 2010), 14 m (Bayoglu Flener 2010) and 10 m

(Brachman *et al.* 2010) span box culverts were tested to failure. Earlier in 1970, a 6.3 m span pipe arch (Klöppel and Glock 1970) was tested to failure under a uniformly distributed load (meant to represent railway load). A smaller 3.8 m span pipe arch was also tested to failure during the 1980s (Temporal *et al.* 1985) under a single axle load. An ellipse of a 1.6 m span was recently tested to failure under a tandem axle load (Regier *et al.* 2017). Moreover, in the late 1980s, a series of extensive field tests were carried out on a 6.1 m span pipe arch culvert (see Figs. 1-2) in Enköping, Sweden (Pettersson 2007). The full-scale test involved the structural performance during backfilling, under live load, and loading to failure (see Fig. 1). This case study was motivated for this particular investigation for being, to the authors, one of the largest loading to failure tests performed on a regular metal culvert (i.e., not box culvert) under a single axle load, and also for its extensive testing program. The pipe arch was fabricated from 200×55 mm corrugated steel plates (see Fig. 3) with a thickness of 3.25 mm for the crown plates (between 65° crown angle) and 2.95 mm for the remaining plates (the different thicknesses were due to crown plate replacement subsequent to the different failure tests) (Pettersson 2007).

Conduit deformations, steel wall strains, and soil pressures, were monitored and measured. While live load

Fig. 1 Enköping pipe arch, loading to failure test. Steel weights were used to increase the load on the axle simulating the live load
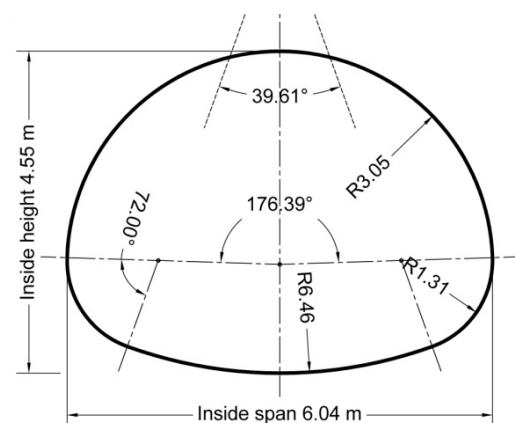

Fig. 2 Enköping pipe arch dimensions (m). Radii are to center line of the corrugated wall

tests were performed for different soil covers, the loading to failure tests were performed for 0.75 m depth of soil cover. Several compaction levels were studied in the live load tests as well as in the ultimate tests. The loading rig for the ultimate load test was built to represent a single axle load with two footprints of 0.2×0.6 m separated by a 2 m distance centre to centre. The footprints were fabricated to represent the defined wheel loads in the Swedish bridge code at the time of the test. The width of the tested pipe was 5 m and the axle load for the ultimate test was placed on the soil directly above the crown (i.e., 2.5 m represents symmetry plane). Moreover, the field test had two additional pipe segments (separated from the main 5 m pipe) on each end to facilitate the test boundary conditions (Pettersson 2007).

The backfilling soil was classified to the unified soil classification system as "SP" poorly graded gravely sand. During the backfilling, three plate bearing tests were performed on the compacted soil. While the first test showed secant moduli of 56 MPa and 107 MPa for the first and second load cycles respectively, the second plate bearing test resulted in higher secant moduli of 74 MPa and 176 MPa for the first and second load cycles respectively (Pettersson 2007). The ultimate tests were performed for three compaction levels being 85%, 92%, and 94% modified Proctor. The paper will focus on the field measurements reported for the 92% compaction case. The steel material was tested and an average yield stress of 350 MPa was reported and a mean elastic modulus of 203 GPa was evaluated. More details on the different instrumentations, testing program and field results can be found in (Pettersson 2007).

3. Numerical simulation

3.1 General

This investigation was performed using the FEM program Abaqus (Dassault Systemes SIMULIA Corp. 2017). In order to capture the failure load of the test, proper material models and different associated input parameters had to be assumed. The process of reaching a calibrated 3D model to field measurements is explained throughout the study in several simulation attempts of which each represent different input parameters for the backfilling soil. The inclusion of different simulations results was meant to separate the influence of the different input soil parameters on the structural response. Although, plate bearing tests were performed on the backfill soil, the outcome of these tests does not provide complete data for the soil as in the case of the chosen Mohr-Coulomb material model. It is important to highlight that the soil parameters were not determined from a specific soil testing but were based initially on simple correlations and further changed to reasonably fit the field measurements. The backfill soil inputs including elastic modulus and peak friction angle were altered from their starting assumptions until reaching an acceptable calibrated model. More details on the different assumptions and the calibration procedure are described in the following sections.

3.2 Study outline

The methodology of the paper involves assuming initial soil parameters for a first (SIM01) fully elastic model (soil and steel), where the soil elastic moduli are initially assumed based on Duncan-Chang's approach (Duncan and Chang 1970) for tangent modulus calculation. Thereafter, a second model (SIM02) was generated using the same values of soil moduli but with the introduction of soil plasticity using a Mohr-Coulomb material model. The initial value of peak friction angle was assumed based on the calculation approach presented by Pettersson and Sundquist (2014) using the sieve analysis and the density of the backfill material that were reported by Pettersson (2007). Three other simulations (SIM03-05) were additionally evaluated by altering the backfill soil parameters (elastic modulus and peak friction angle) and keeping the initial assumptions for the native soil until reaching a reasonable calibrated model for the ultimate failure field test. SIM06 was based on the same input parameters of SIM05 but with the change of the interface between the steel and soil materials to a tied interface (see Section 3.4). For all these six models (SIM01-SIM06), the steel material was assumed elastic. The results of the first six simulations were analysed and discussed compared to the field measurements. In order to numerically capture the failure load of the test, the yield limit for the steel pipe material was introduced in a new (7th model, SIM07) using the same input parameters as in the latest calibrated model (SIM06). The 7th model also included the initial stresses in the pipe from the backfilling process prior to applying the axle load increments. The inclusion of pipe stresses from backfilling is important to properly capture a realistic formation of the plastic hinges in the pipe. Details on the different assumptions and inputs are treated in the next sections of the paper.

3.3 Model configuration

The presence of two planes symmetry was utilized upon building the model. The soil mass around the steel pipe was
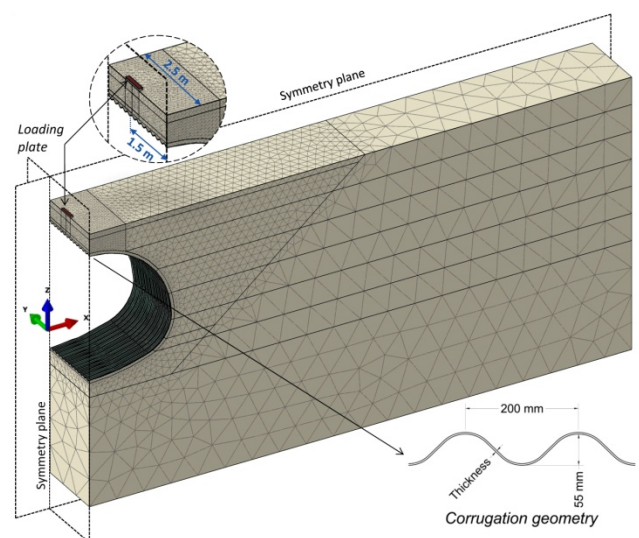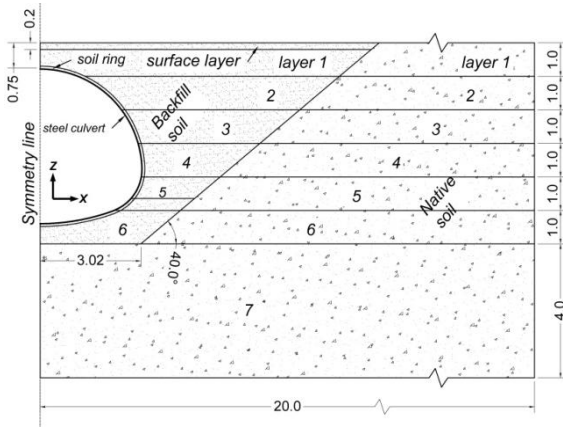

Fig. 3 View of the 3D model

Fig. 4 Schematic of model details and dimensions (m)

divided into backfill and native soil volumes (Figs. 3-4). Both soil volumes were divided into 1 m thick layers to allow for different definitions of the soil parameters, where soil elastic modulus was set to increase with depth (see Section 3.4). The geometry of the native and backfill soils was assumed based on details in (Pettersson 2007) as shown in Fig. 4. The corrugation of the steel pipe was modelled explicitly. This choice is motivated to avoid any unnecessary uncertainties, and considering what other study Elshimi (2011) has showed that explicit modelling of the corrugation is important especially for the case of ultimate loading. The axle load was applied using displacement control of an assumed 50 mm thick steel plate on the soil surface (see Fig. 3). This plate had the dimension of a wheel footprint (see Section 2.0) being 0.2 × 0.6 m (i.e., 0.1 × 0.6 m because of the symmetry).

3.4 Assumptions and input parameters

In order to assume a proper increase of the soil elastic modulus with depth, the starting values were calculated (see Section 3.2) based on Duncan-Chang's equation (Duncan and Chang 1970) for tangent modulus E_t as illustrated in Eq. (1).

$$E_t = \left[1 - \frac{R_f(1 - \sin\varphi)(\sigma_1 - \sigma_3)}{2c\cos\varphi + 2\sigma_3\sin\varphi}\right]^2 K p_a \left(\frac{\sigma_3}{p_a}\right)^n \quad (1)$$

The equation presumably captures the increased effect

of the confinement pressure σ_3 on the soil moduli values, where σ_3 was calculated for the different depths based on assuming at-rest soil pressure coefficient $K_o = 1 - \sin\varphi$ As stated in Section 3.2, the initial value of the peak friction angle φ was calculated based on the method presented by Pettersson and Sundquist (2014) and using a soil density $\rho_{soil} = 17.8$ kN/m^3 and a standard Proctor compaction $RP^{std} = 97\%$ (using the rule of thumb, standard Proctor = modified Proctor + 5%) (Pettersson 2007). The reported sieve analysis (Pettersson 2007) gave a uniformity coefficient $C_u = 3.3$ and $d_{50} = 0.91$ mm. By using these input values, the method (Pettersson and Sundquist 2014) calculates a friction angle $\varphi = 36°$. The method also calculates modulus a number $K = 1003$ and an exponent $n = 0.47$ that are also needed for the initial evaluation of the tangent modulus in Eq. (1). The failure ratio R_f was set to 0.7 (Duncan and Chang 1970) and the backfill soil cohesion c was set to 3 kPa. This small cohesion value was used to facilitate unnecessary convergence issues. The major stress σ_1 is the weight of soil column at each soil layer and p_a is the atmospheric pressure being 100 kPa. Hence, Eq. (1) returned initial values of tangent modulus E_t as shown in Table 1 (i.e., SIM01). Although these values may be considered relatively low, they were used as the opening assumptions for the first elastic model simulation (i.e., SIM01 in Table 1). Concurrently, design values of soil modulus are normally conservative as one may compare with a recommended design value of secant modulus from (CSA Canadian Standards Association 2014) being 27 MPa (SP soil, 97% standard Proctor) and a calculated characteristic value of tangent modulus from (Pettersson and Sundquist 2014) being 14 MPa. To reach a reasonable calibrated model with the field measurements, and for the next simulations, these values were simply increased by some factor. As Table 1 shows, the used factors for the increase of tangent modulus were deliberately assumed to achieve a backfill soil modulus of 55 MPa and 100 MPa for the first backfill layer (i.e., 1 m), which are comparable to the reported modulus from the plate bearing tests (see Section 2.0). Table 1 also presents the assumed peak friction angle φ for the different simulations. One may note the presence of a 0.2 m deep surface layer which had a higher peak friction angle and cohesion (i.e., SIM02 and SIM03) than the rest of the backfill layers. The reason for this was to allow a higher load application and to avoid a premature calculation termination at a low load due to soil failure. The

Table 1 Input parameters of the backfill soil for the different simulations

Soil layer/Simulation		SIM01	SIM02		SIM3		SIM04		SIM05		SIM06	
Layer	Width (m)	E_s (MPa)	E_s (MPa)	$\varphi°$	E_s (MPa)	$\varphi°$	E_s (MPa)	$\varphi°$	E_s (MPa)	$\varphi°$	E_s (MPa)	$\varphi°$
0	0.2	13	13	45	55	45	55	45	100	49		
1	0.8	13	13	36	55	36	55	45	100	49	Same values as SIM05. The interface between the steel pipe and the backfill soil is changed to a tied interface.	
2	1.0	17	17	36	76	36	76	45	138	49		
3	1.0	21	21	36	92	36	92	45	167	49		
4	1.0	24	24	36	105	36	105	45	191	49		
5	1.0	27	27	36	116	36	116	45	212	49		
6	1.0	29	29	36	127	36	127	45	230	49		

cohesion *c* of this surface layer was set to 10 kPa, while the remaining backfill layers had a cohesion value of 3 kPa. The native soil parameters were fixed for all the six simulations by having the same input values in SIM01 and SIM02 for the elastic model and plastic models respectively. The native soil had no subsurface layer of 0.2 m of higher values of φ and *c* (see Fig. 4). The cohesion for the native soil was assumed 5 kPa for all the plastic soil simulations (i.e., SIM02-06). The dilation angle ψ of soil was assumed to follow $\psi = \varphi - 30^o$ (Plaxis bv 2016). The lowest layer (7th) of the native soil (see Fig. 4) had a soil modulus of 33 MPa for all the simulations SIM01-06. The soil elastic modulus and peak friction angle of the soils are assumed to be constant throughout the analysis of each simulation. Geometric nonlinearities were only considered in SIM07. Poisson's ratio for both the soil and steel materials was set to 0.3. Primarily, the interface between the steel pipe and the soil was modelled using a frictional contact with a friction coefficient $\mu = 0.4$. The assumed friction coefficient was based on a suggested value for the interface between steel and gravel-sand mixtures (Bowles 1997). This value was kept unchanged for simulations SIM01-05 of the frictional interface regardless of the change in the backfill peak friction angle.

During the calibration process, it was evident that it would require a very high value of the backfill peak friction angle (higher than 55°) to reach a reasonable calibrated model with the field measurements. This raised a concern of assuming unrealistic peak friction angle knowing that the used backfill material was classified as poorly graded gravely sand. Therefore, it was decided to keep upper values for the backfill peak friction angle and the 1st layer modulus being 49° and 100 MPa respectively. Consequently, a reasonable calibrated model (SIM06) was achieved using these upper values by changing the interface between the steel pipe and the soil materials to a tied (i.e., no slip) interface (see Table 1). Furthermore, a more detailed study on the effect of having tied and frictionless interfaces was also included and compared for the elastic model SIM01 (see Section 4.5).

The soil was modelled using quadratic tetrahedral solid elements of type C3D10 and the steel pipe corrugation was modelled using linear quadrilateral shell elements of type S4R. The global mesh size for the steel pipe was 3 cm with 1 cm mesh refinement along the corrugated curves. The global mesh size for the soil was 1 m with 30 cm refinement of the backfill soil. The soil ring (≈ 0.1 m thick) around the pipe had a mesh size of 10 cm and the same size was used for the soil volume above the crown (compare Fig. 3). The model had around 1.8 million degrees of freedom. While symmetry boundary condition was applied of two vertical surfaces in the X and Y directions (Fig. 3), all the other vertical surfaces were restrained in the horizontal direction. Symmetry boundary conditions were applied to the corrugated steel shell on the sides of X and Y symmetry planes (Fig. 3). The remaining side of the shell was left free from any restraints, which correspond to the actual field configuration (Pettersson 2007). The movement of the bottom soil surface was restrained in all three directions. The effect of soil confinement was checked by running the

elastic model (SIM01) with no horizontal restraints on the backfill soil side (the side where there is no symmetry plane). The lateral soil movements due to live loading were seen very small and there was no noticeable effect on the structural response of the pipe.

In order to predict the ultimate failure load, a new model (SIM07) was created based on the last calibrated model (i.e., SIM06) with the inclusion of steel plasticity. The steel yield strength of 350 MPa was defined at strain level of 0.17% (Pettersson 2007). Typically, each simulation started with a step where the native soil only was activated (see Fig. 4) and geostatic soil stresses were generated. A lateral earth pressure coefficient of 0.41 was assumed which corresponds to at-rest earth pressure of 36° friction angle (1-sin 36°). The second step involved the activation of the backfill soil together with the pipe, where the dead weights of soil and pipe were applied. The next steps dealt with the application of axle loads (SIM01-06). In SIM07 the stresses induced by backfilling were generated followed by the application of axle loads.

4. Results and discussion

This section presents the results from simulations SM01-SIM06. The section also includes the results from SIM07, where pipe stresses induced by backfilling and steel plasticity are introduced (see Section 3.4). The structural response including deformation, normal forces and bending moments is compared to the reported field measurements. Stresses in the soil are also compared to field cell pressure readings. While the structural response of the crown section (i.e., under the wheel load) is the main focus, the distribution of section forces along the pipe circumference is also presented and discussed. For all the six simulations, the intention was to have the applied axle load exceeding 500 kN, since field failure was observed at 524 kN (Pettersson 2007). Yet, SIM02 and SIM03 having low peak friction angles were terminated at a lower axle load as they had reached a state close to soil failure. The results from the remaining simulations (i.e., SIM01, SIM04-06) were reported up until an axle load of about 500 kN (for instance see Fig. 5). For the elastic steel models (i.e., SIM01-06), the normal forces and bending moments were calculated using the extracted stresses from the extreme top and bottom fibres of the corrugation. It is worth mentioning that the legends in the results figures - where applicable - are designated by the soil elastic modulus of the first top backfill layer (see Fig. 4 and Table 1). The assumed value of the peak friction angle (49°) for models SIM05-SIM07 may be considered high for the given backfill soil. Yet, cohesionless soils could exhibit high values of peak friction angles especially in very dense soils (Simoni and Houlsby 2006). In any case, the basic representation of the Mohr-Coulomb material model for the soil together with the assumed interface are believed to be important factors affecting the final assumptions of the reached calibrated model. Moreover, the change of the interface assumption in SIM06 was needed to reach the final calibrated model under reasonable assumptions of the backfill input parameters.
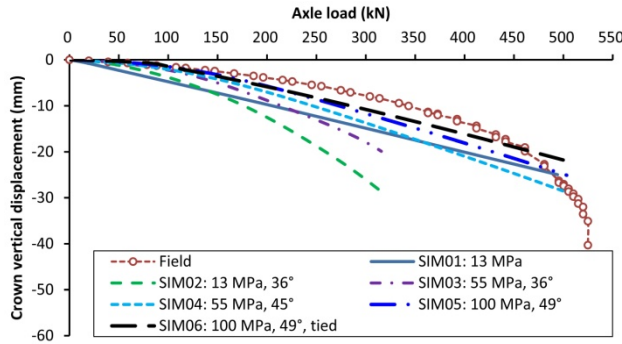
Fig. 5 Vertical displacement of the crown point

Fig. 6 Bending moment of the crown point

Fig. 7 Bending moment distribution along the pipe circumference as extracted at an axle load of 221 kN

This may be justified that the tied interface was needed to compensate for the choice of the simplified Mohr-Coulomb material model for the studied case particularly under the extreme loading. In such an elastic-plastic material response, a tied interface implies that the shear strength of the interface is limited to the shear strength of the backfill soil. With that in mind, previous studies (Duncan 1979, Mohammed and Kennedy 1995, Elshimi *et al*. 2013) have suggested that flexible culverts would expectedly have a minimal slip between the soil and the steel materials. This could be reasonably said for culverts built with well-compacted backfill and under normal levels of live loads.

4.1 Displacements

The crown point deflection was extracted and compared to field measurements for all the seven simulations (see Table 1). Fig. 5 shows the deflection versus the axle load for the different simulations. One may note that although that the elastic model (SIM01) had a softer response when compared to field data, yet it provided a good prediction for the deflection at higher axle load (i.e., near failure load). Obviously, the increase in elastic modulus and peak friction angle of the backfill soil plays an important role in decreasing the crown deflection. Hence, for the same elastic soil modulus and at about 250 kN axle load, Fig. 5 shows that a 25% increase of the backfill peak friction angle (SIM03 and SIM04) did obviously reduce the crown vertical displacement by around 21%. On the other hand, increasing backfill elastic modulus by 330% (SIM02 and SIM03) ended up with a reduction in crown vertical displacement by about 30% at an axle load of 250 kN. Fig. 5 also shows that SIM06 with the assumption of backfill peak friction angle of 49°, an elastic soil modulus of 100 MPa (1st layer) and a tied interface provided a good estimate of the crown deflection for the tested structure. Similar results were observed when looking at other structural responses as described in the following sections.

4.2 Bending moments

Fig. 6 shows the bending moment distribution at the crown point directly below the applied load. One may note that the elastic model (i.e., SIM01) provided a good estimate for the crown bending moment up to about 400 kN axle load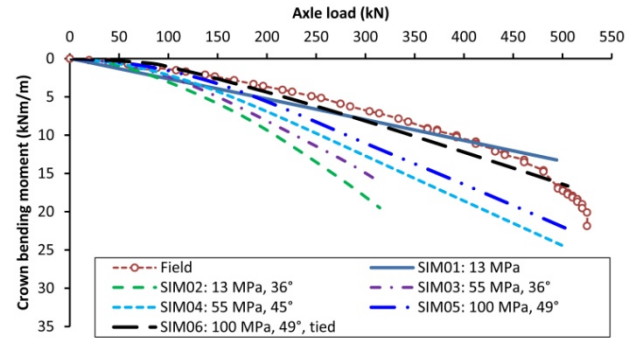. Th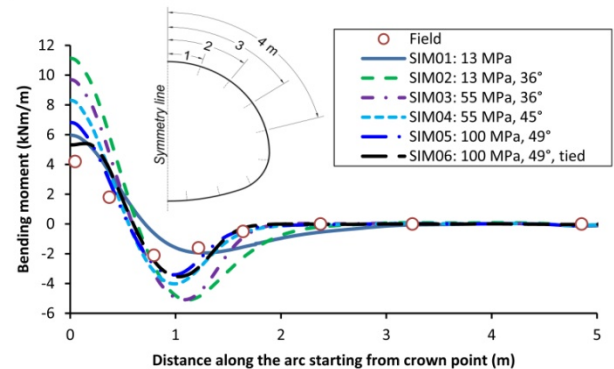e effect of soil modulus increase is clearly seen between SIM02 and SIM03, where if looking at 200 kN axle load, a 330% increase in soil modulus resulted in 13% decrease in crown bending moment. While the influence of the peak friction angle can be realized between SIM03 and SIM04, where similarly at 200 kN axle load, a 25% increase in the peak friction angle resulted in about 14% reduction in the crown bending moment. The distribution of bending moments along the pipe circumference was also extracted and compared for the different simulations as illustrated in Fig. 7. The values were extracted at about 221 kN axle load. Fig. 7 indicates that all the simulations had the same trend of bending moments along the pipe circumference, yet one may note that the elastic model (SIM01) did not capture well the bending moment trend at negative values. On the other hand, Fig. 6 shows the significant influence of the tied interface when SIM06 is compared to SIM05. Fig. 6 also shows that SIM06 describes reasonably well the bending moment response compared with the field measurements.

4.3 Normal forces

The estimation of live load normal forces in design methods does not normally depend on the soil elastic modulus (CSA Canadian Standards Association 2014, Pettersson and Sundquist 2014). However, the results of this study shows slight differences regarding this assumptions, where Figs. 8-9 illustrate that changing the elastic modulus of backfill soil may have an influence on the live load normal forces especially around the crown area (compare
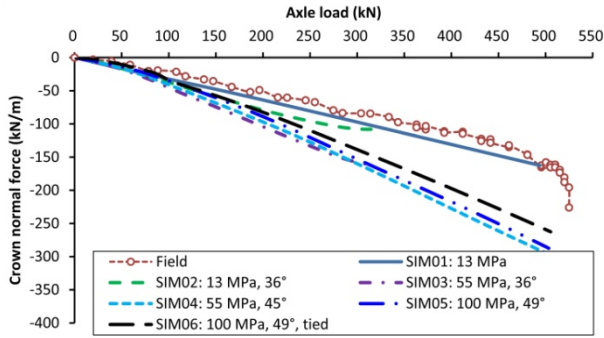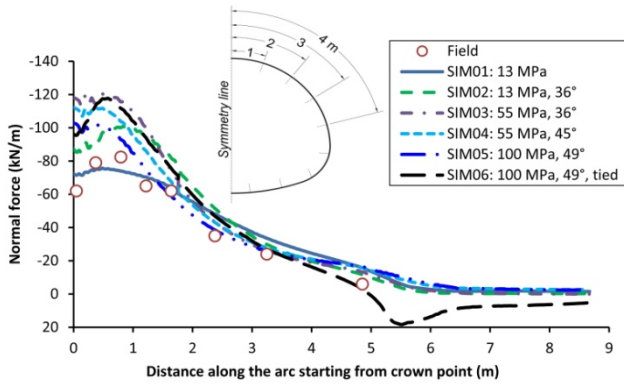
Fig. 8 Normal force of the crown point

Fig. 10 Live load vertical pressure extracted at 0.15 m above the crown

Fig. 9 Normal force distribution along the pipe circumference as extracted at an axle load of 221 kN

was compacted to 92% modified Proctor), the assumption of the soil as an elastic medium (i.e., Boussinesq's) for live load stress distribution can be reasonable for design purposes (Pettersson and Sundquist 2014). However, Fig. 10 also shows that at high loads, the efficiency of soil in distributing the live load stresses is reduced, where the shear capacity of soil is largely utilized (compare SIM05). Obviously, the peak friction angle of the soil seems to have a major influence on the distribution of live load stresses in the soil, where a higher peak friction angle tends to reduce the live load stresses in soil (compare SIM03-04). In relation to that, one may note that a good compaction (i.e., increasing the relative density) will not only increase the soil elastic modulus but will also enhance the friction angle of soil (Mayne 2006). It may be noticed that the field measurement in Fig. 10 shows a bounce, which nearly coincides with the 1st yielding of the pipe wall (see also Section 4.6). It is interesting to note that SIM06 resulted in lower live load vertical stresses compared to SIM05, which may be attributed to the change of the overall stiffness resulted by the change of the interface.

SIM02 and SIM03). A similar observation was noted by Moore and Brachman (1994) based on fully elastic analyses. On the other hand, Figs. 8-9 show that the increase of the peak friction angle tends to reduce the resulting normal forces (i.e., SIM 03 and SIM04) and this reduction is more obvious all along the pipe circumference. This effect is believed to be attributed to the change in load distribution through the soil resulting from the change in the peak friction angle. One may also observe that the change to a tied interface (SIM05 and SIM06) has a noticeable influence on the distribution of normal forces as clearly seen in Fig. 9. Similar to previous studies (Moore and Brachman 1994, El-Sawy 2003), the choice of a tied interface resulted in small tension forces at the bottom part of the pipe.

4.5 The effect of interface choice

The influence of having tied and frictionless interfaces between the soil and steel materials was further investigated and compared to the assumed frictional interface using the elastic model SIM01. The comparison was made by looking

4.4 Stresses in soil

The field test had pressure cells in the soil mainly placed around crown area of the buried pipe. The field readings from a pressure cell located vertically under the wheel load and at 0.15 m above the crown (i.e., at 0.6 m soil depth) were compared to the results from the different simulations. Fig. 10 shows the live load vertical stresses in soil in comparison to the reported field measurements. It is interesting to note that the field measurement stresses are close to the theoretical stress line as evaluated by Boussinesq's theory (Das 2006). This naturally indicates that when soil is well compacted (the backfill soil in the test
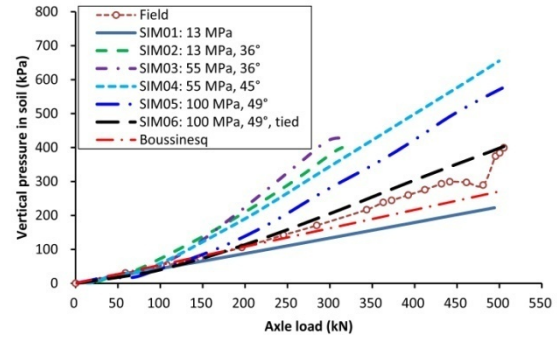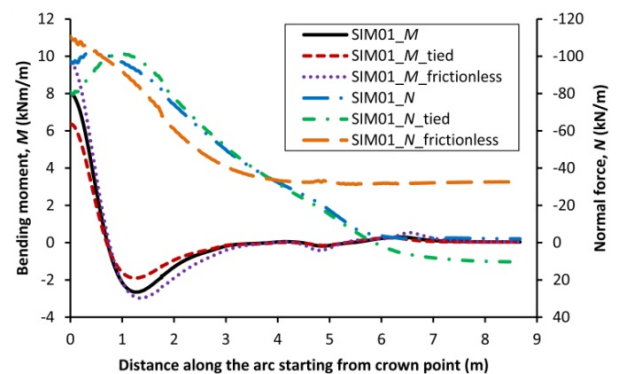

Fig. 11 Sectional forces comparison for tied, frictionless and frictional interface choice shown for SIM01. Shown at 300 kN axle load

at the distribution of sectional forces along the pipe. Fig. 11 illustrates that in a numerical simulation, adopting a tied interface will clearly reduce the live load effects in the conduit wall, while a frictionless interface will increase them. This distinction is particularly seen at the crown area. For instance, when comparing to the assumed frictional interface, for the tied interface, the crown normal force is less by 17%, and the crown bending moment is less by 20%. For the frictionless interface, the crown normal force is increased by 13%, whereas crown bending moment is increased by 20%. Therefore, the influence of interface choice is clearly an important factor and should be carefully thought through specially when simulating ultimate capacity of SSCB.

4.6 Prediction of failure load

In order to reasonably estimate the failure load of the tested structure, the pipe stress state induced by the backfilling soil had to be taken into account. Normally, the backfilling operations of flexible culverts induce relatively large bending stresses in the culvert wall. A negative bending moment (tension in top fibre) would normally occur at the crown area and a positive one around the quarter point. In any case, since the backfilling stresses are normally significant, it becomes essential to include those to properly predict the actual stresses in the conduit wall especially upon yielding. Therefore, SIM07 model was generated (see also Sections 3.2 and 3.4) based on the last calibrated model SIM06 with the modification of defining a plastic steel material and the inclusion of the pipe stress state from the backfill soil. The 3D simulation of the backfilling stresses can be a computational demanding process as one may need to include all the backfill layers and compaction effects (Wadi *et al*. 2015, 2016). Instead, the pipe stresses from the backfilling were achieved by applying a distributed prescribed displacement on the soil ring around the pipe (see Fig. 12). The magnitude and the distribution of this displacement were approximately
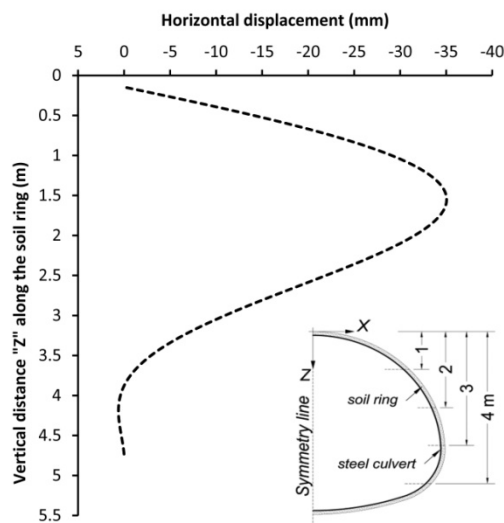
derived from a simplified equivalent 2D model. This displacement was applied at once after the completed backfill and then deactivated in the next analysis step prior to applying the axle load increments. In overall, the idea was to induce a stress state in the pipe similar to the field measurements before the application of the axle load. Fig. 13 shows a comparison between the induced soil stresses along the pipe circumference by this technique as compared to the calculated values from the field test. The induced stresses by this technique are in good agreement with the calculated stresses from the field measurements. It should be noted that Fig. 13 shows the backfill field stresses as calculated from three different sections along the pipe, which explains the scatter and in some cases the different values of stress even for the same location. By the end of backfilling, the field measurements reported an average value of crown bending moment of about -9 kNm/m, and an average upward crown vertical displacement of 60 mm (Pettersson 2007).

Fig. 14 shows a comparison of the crown vertical deformation between the field measurements and the simulation attempt SIM07. The figure shows a clear overestimation of the failure load in comparison to the field response. Yet, it is interesting to note the 1st yield area from SIM07 occurs at about 420 kN axle load and that is closely coinciding with the strain field measurements (1st field yield is believed to have occurred at about 480 kN axle
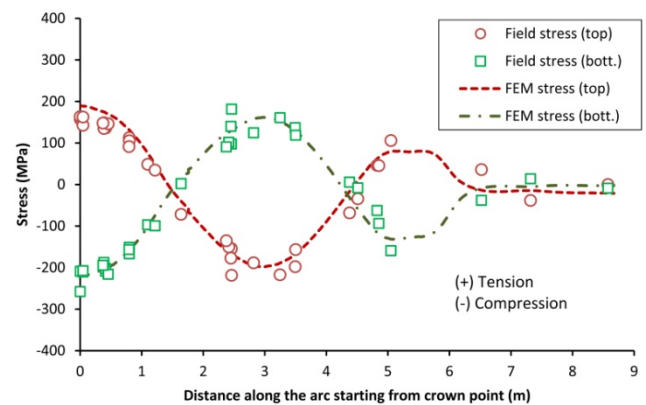

Fig. 13 Field soil stresses along the pipe circumference as compared to the induced values from FEM

Fig. 12 Distribution of the prescribed horizontal displacement to simulate the desired stress state from the backfilling
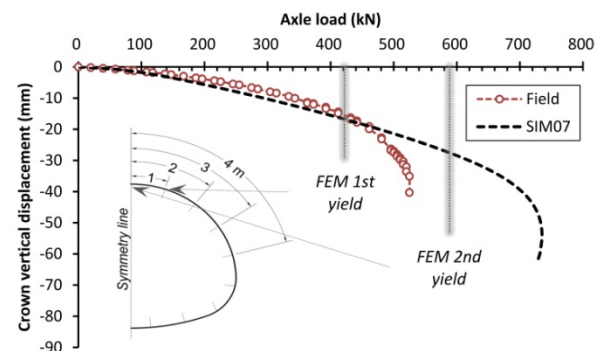

Fig. 14 Crown vertical displacement comparison for ULS simulation and field measurements

load) when looking at one strain gauge located at the bottom of corrugation at about 0.8 m arc distance from the crown. The total stresses (from backfill plus axle load) along the pipe circumference were extracted from SIM08 at 460 kN and plotted against the calculated field values from measurements as shown in Fig. 15. The reason for selecting 460 kN axle load (instead of 480 kN) is that the one concerned strain gauge (believed where 1st yield area occurred) had reported bad readings above 460 kN axle load.

The 1st yield area appears to occur at about 1 m from the crown line, where the bottom fibre is yielding in compression (see Figs. 15-16). The total FEM stress distribution along the pipe circumference shown in Fig. 15 is in good agreement with the calculated values from field measurements. Fig. 15 also shows a stress peak from the FEM results which was closely captured by the field instrumentation. It should be noted that the field stresses in Fig. 15 are calculated from two different sections along the pipe, where they represent the two instrumented sections under the two footprints of the applied axle load. Although that live load bending moment is a maximum at the crown (compare Fig. 7), the 1st yield area did appear
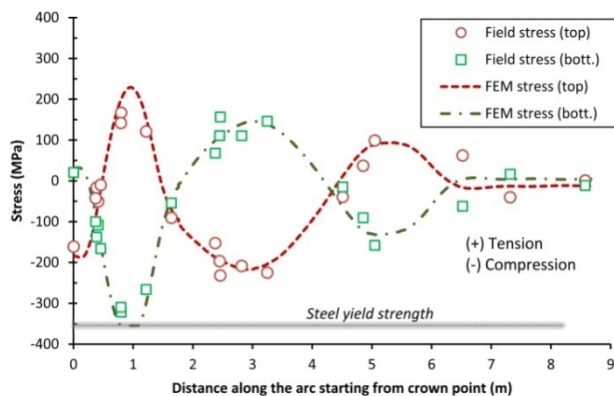

Fig. 15 Total stress comparison along the pipe circumference shown at about 460 kN axle load
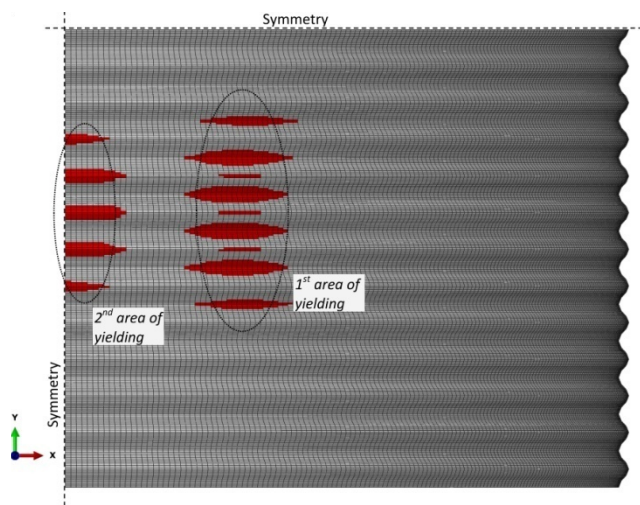

Fig. 16 Location of 1st and 2nd areas of yielding (based on von Mises stresses)

away from the crown area. This is referred to the stress state from the backfilling (mainly the bending moment), where a high negative moment already exists at the crown area prior to the start of the live loading process. The build-up of the negative bending moment together with the normal force at about 1 m from the crown area has caused the 1st yielding at that specific location, whereas the subsequent formation of the 2nd yield area at crown area is due to the presence of large backfilling negative moment at the crown.

The results form SIM07 suggests that the failure of the tested pipe was mainly caused by the formation of three-point plastic hinges mechanism under high normal forces and bending moments. The same conclusion was attributed to the results of the field test itself (Pettersson 2007). SIM07 also shows that the load penetrated the soil surface about 31 mm at 460 kN axle load and about 82 mm at the 730 kN failure axle load. Fig. 17 also shows the evolution of the live load vertical stress in the soil as extracted (from SIM07) at 0.6 m below the soil surface. It is interesting also to see how the ratio (calculated as ratios of the applied surface pressure) of live load stress does increase with the increase of axle load. The stress ratio from Boussinesq theory is already exceeded for axle loads bigger than 200 kN, where it indicates that the shear capacity of the soil is largely mobilized prior to the numerically predicted failure load in SIM07. In any case, the overestimation of FEM failure load in comparison to field testing as shown in Fig. 14 is an interesting result. Of course the limitations in the presumed material model for soil have some influence, where the assumed Mohr-Coulomb material model is a modest idealization of how soils behave specially at extreme loading. Yet, the field measurements show that after the presumable formation of 1st yield area and unlike the ductile behaviour resulted in the FEM simulation, there was a quick reduction in the structural stiffness, which prompted a quicker failure (Fig. 14). In reality, these culverts are fabricated from multi-plates which are curved and bolted together to the desired shape. In this study, the pipe was modelled as a continuous plate, where the bolted connections have been neglected.

The tested structure had one of the bolted connection right at the crown area, where the 2nd yield area is believed to have occurred (see Fig. 18). The manner of how stresses
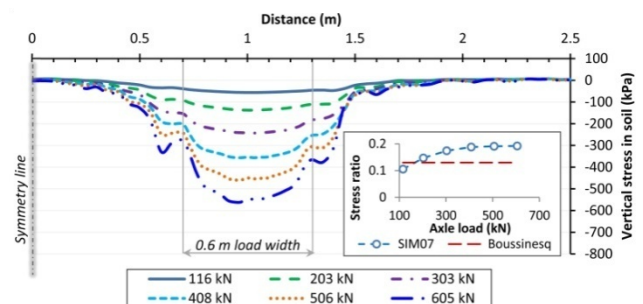

Fig. 17 Live load vertical stresses in the soil extracted at 0.6 m depth for different values of axle loads of SIM07. The stress ratio is calculated for each showed axle load as (average stress within 0.6 m width)/(applied surface pressure)
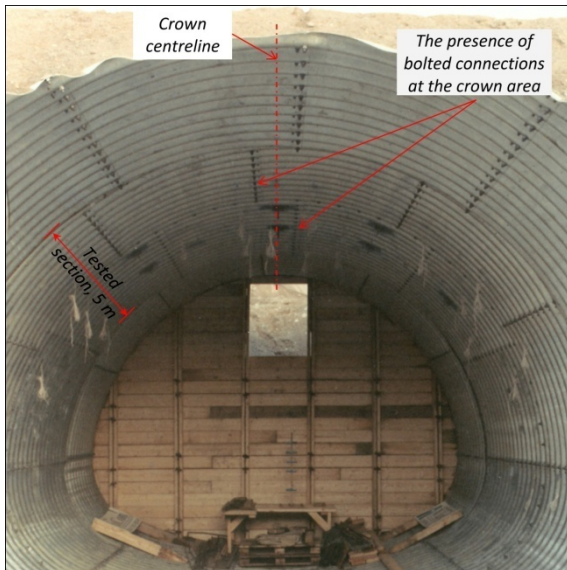
Fig. 18 An inside snapshot of the tested culvert
showing the upper crown area

are transferred from plate to plate in a bolted connection could have a considerable influence of how the structures behave especially in post yielding. Furthermore, and in a previous study (Klöppel and Glock 1970), bolted connections were tested under increased normal forces having different eccentricities (i.e., $e = M/N$). These tests showed that bolted connections can have a considerable influence on the structural response of the corrugated plate, where it directly affects the evolution and definition of the elastic and the ultimate capacity accordingly. In some cases, the capacity of the bolted connection can be approximately equal to the bending moment at first fibre yielding for the corrugated steel plate. Therefore, one may supposedly say that if the bolted connection behaviour was taken into account, the FEM simulation would have a failure load at approximately the 2nd area of yielding as shown in Fig. 14.

5. Conclusions

In this study, the use of 3D FEM has been utilized to provide deeper insights about the structural behaviour of a corrugated pipe arch case under extreme single axle loading. The influence of different backfill soil inputs including soil elastic modulus and peak friction angle has been investigated and discussed, where live load deformation, normal forces and bending moments were analysed and compared to field measurements. In addition, the effect of the interface choice including frictionless, frictional or tied interface between soil the steel was studied and discussed.

- The study shows that despite the composite nature of flexible culverts, numerical simulations can be efficient in capturing their performance under live loading. However, results of such method should be always perceived in conjunction with the assump-

tions and the limitations involved in the modelling process. Although, a calibrated model was achieved for the given range of loading, the model resulted in an overestimation of failure load compared to field data, whereas reasons beyond this outcome were arguably presented and discussed.

- The opening assumption of the soil elastic modulus (an average backfill modulus of 22 MPa) in a fully elastic model resulted in a higher crown deflection compared to field measurements. The elastic model also calculated a relatively higher crown bending moment up until about 400 kN axle load. However, the crown normal forces were very close to the measured values from the elastic model.

- The increase in the backfill soil peak friction angle had a major influence on reducing the live load pressure in the soil and subsequently reducing the live load effects in the pipe wall. On the other hand, the increase of the backfill soil elastic modulus did seem to influence the normal forces in the pipe, which was more observed in the crown area.

- The study also showed that it would require a larger increase in the soil elastic modulus than the friction angle to achieve a similar reduction of displacement and bending moments.

- The choice among frictionless, frictional, or tied interface can have a considerable influence on the live load effects and should be thought through when modelling SSCB. However, the limitations induced by the use of a simplified soil material model (i.e., Mohr-Coulomb) may delimit the assumptions regarding the interface choice between the steel and soil materials especially at extreme loading.

- The complex nature of the interaction between the soil and steel materials was experienced when attempting to estimate the failure load of the tested culvert. Obviously, the stresses from the backfilling soil play an important role in defining the subsequent formation of yield areas.

- Although a calibrated model has been achieved for the given loads, yet the calibrated model overestimated the failure load. This overestimation was mainly believed due to the limitations in the assumed soil material model and more importantly the fact that the model neglected what is believed to be a critical presence of a bolted connection at the crown area.

The results of this study clearly emphasize the importance of the proper characterization of the backfill soil material. It is strongly believed that the adequate testing of the backfilling soil material is a crucial part for any full-scale testing program of SSCB, especially when performing loading to failure tests. A comparison of different soil material models on the ultimate capacity of a SSCB could certainly be an interesting topic for future studies. The proposed arguments about the influence of the bolted connections on the ultimate capacity of SSCB could be part of future studies, where the structural behaviour of various curved corrugated plates is closely investigated.

Acknowledgments

References

AASHTO (2012), LRFD Bridge Design Specifications, American Association of State Highway and Transportation Officials; Washington, DC, USA.

Bayoglu Flener, E. (2010), "Testing the response of box-type soil-steel structures under static service loads", *J. Bridge Eng.*, **15**(1), 90-97.

Bayoğlu Flener, E. and Karoumi, R. (2009), "Dynamic testing of a soil-steel composite railway bridge", *Eng. Struct.*, **31**(12), 2803-2811.

Beben, D. (2013), "Field performance of corrugated Steel plate road culvert under normal live-load conditions", *J. Perform. Constr. Facil.*, **27**(6), 807-817.

Beben, D. and Stryczek, A. (2016), "Numerical analysis of corrugated steel plate bridge with reinforced concrete relieving slab", *J. Civil Eng. Manag.*, **22**(5), 585-596.

Beben, D. and Wrzeciono, M. (2017), "Numerical analysis of steel-soil composite (SSC) culvert under static loads", *Steel Compos. Struct.*, *Int. J.*, **23**(6), 715-726.

Bowles, J.E. (1997), Foundation Analysis and Design, (5th Edition), McGraw-Hill Companies, New York, USA.

Brachman, R.W.I., Moore, I.D. and Mak, A.C. (2010), "Ultimate limit state of deep-corrugated large-span box culvert", *Transport. Res. Record*, **2201**, 55-61.

CSA Canadian Standards Association (2014), Canadian Highway Bridge Design Code S6-14, (11th Edition), CSA Canadian Standards Association; Canada.

Das, B.M. (2010), Principles of Geotechnical Engineering, (7th Edition), Cengage Learning, Stamford, USA.

Dassault Systemes SIMULIA Corp (2017), Abaqus 2017.

Duncan, J.M. (1978), "Soil-culvert interaction method for design of metal culverts", *Transport. Res. Record*, **678**, 53-59.

Duncan, J.M. (1979), "Behavior and design of long-span metal culverts", *J. Geotech. Eng. Div.*, **105**(3), 399-418.

Duncan, J.M. and Chang, C.Y. (1970), "Nonlinear analysis of stress and strain in soils", *J. Soil Mech. Found. Div.*, **96**(SM 5), 1629-1653.

El-Sawy, K.M. (2003), "Three-dimensional modeling of soil-steel culverts under the effect of truckloads", *Thin-Wall. Struct.*, **41**(8), 747-768.

Elshimi, T.M. (2011), "Three-dimensional nonlinear analysis of deep-corrugated steel culverts", Ph.D. Dissertation; Queen's University Ontario, Canada.

Elshimi, T.M., Brachman, R.W.I. and Moore, I.D. (2013), "Effect of truck position and multiple truck loading on response of long-span metal culverts", *Can. Geotech. J.*, **51**(2), 196-207.

Klöppel, K. and Glock, D. (1970), "Theoretische und Experimentelle Untersuchungen zu den Traglastproblemen Biegeweicher, in die Erde Eingebetteter Rohre", Institutes für Statik und Stahlbau der Technischen Hochschule Darmstadt, Darmstadt, Germany.

Kunecki, B. and Kubica, E. (2004), "Full-scale laboratory tests and FEM analysis of corrugated steel culverts under standardized railway load", *Arch. Civil Mech. Eng.*, **4**, 41-53.

Mayne, P.W. (2006), "The second James K. Mitchell lecture undisturbed sand strength from seismic cone tests", *Geomech. Geoeng.*, **1**(4), 239-257.

McGrath, T.J., Moore, I.D., Selig, E.T., Webb, M.C., Taleb, B. (2002), "Recommended Specifications for Large-Span Culverts", NCHRP report 473, NCHRP Report, Transportation Research Board, Washington DC, USA.

Mellat, P. andersson, A., Pettersson, L. and Karoumi, R. (2014), "Dynamic behaviour of a short span soil-steel composite bridge for high-speed railways - Field measurements and FE-analysis", *Eng. Struct.*, **69**, 49-61.

Mohammed, H. and Kennedy, J.B. (1995), "Simplified analysis of long-span soil-metal structures", *J. Struct. Eng.*, **121**(10), 1463-1470.

Moore, I.D. and Brachman, R.W. (1994), "Three dimensional analysis of flexible circular culverts", *J. Geotech. Eng.*, **120**(10), 1829-1844.

Moore, I.D. and Taleb, B. (1999), "Metal culvert response to live loading: performance of three-dimensional analysis", *Transport. Res. Record*, **1656**, 37-44.

Pettersson, L. (2007), "Full scale tests and structural evaluation of soil steel flexible culverts with low height of cover", PhD Dissertation, Bulletin 93, KTH Royal Institute of Technology, Stockholm, Sweden.

Pettersson, L. and Sundquist, H. (2014), "Design of Soil Steel Composite Bridges", Report 112, (5th Edition), KTH Royal Institute of Technology, Stockholm, Stockholm, Sweden.

Pettersson, L., Flener, E.B. and Sundquist, H. (2015), "Design of soil-steel composite bridges", *Struct. Eng. Int.*, **25**(2), 159-172.

Plaxis bv (2016), Plaxis 2D Material Models Manual.

Regier, C., Hoult, N.A. and Moore, I.D. (2017), "Laboratory study on the behavior of a horizontal-ellipse culvert during service and ultimate load testing", *J. Bridge Eng.*, **22**(3), 4016131, 1-14.

Simoni, A. and Houlsby, G.T. (2006), "The direct shear strength and dilatancy of sand-gravel mixtures", *Geotech. Geol. Eng.*, **24**(3), 523-549.

Simpson, B., Hoult, N.A. and Moore, I.D. (2015), "Distributed sensing of circumferential strain using fiber optics during full-scale buried pipe experiments", *J. Pipeline Syst. Eng. Practice*, **6**(4), 4015002, 1-10.

Temporal, J., Barratt A.D. and Hunnibell, B.E.F. (1985), "Loading Tests on an ARMCO Pipe Arch Culvert", TRRL Research Report, England, 28 p.

Wadi, A., Pettersson, L. and Karoumi, R. (2015), "Flexible culverts in sloping terrain: numerical simulation of soil loading effects", *Eng. Struct.*, **101**, 111-124.

Wadi, A., Pettersson, L. and Karoumi, R. (2016), "Flexible culverts in sloping terrain: numerical simulation of avalanche load effects", *Cold Regions Sci. Technol.*, **124**, 95-109.

White L.H. and Layer P.J. (1960), "The corrugated metal conduit as a compression ring", *Proceedings of the 39th Annual Meeting of the Highway Research Board*, Washigton DC, USA.

Yeau, K.Y., Sezen, H. and Fox, P.J. (2014), "Simulation of behavior of in-service metal culverts", *J. Pipeline Syst. Eng. Practice*, **5** (2), 4013016, 1-8.

CC